

Electrical Transport Study of Sodium Metaborate: NaBO_2

Kripa Mani Mishra¹, Praveen Kumar Pandey², Gargi Tiwari³, Fozia Zia Haque⁴

^{1,2}Department of Physics, Deen Dayal Upadhyaya Gorakhpur University, Gorakhpur, Uttar Pradesh, India

³Department of Physics, Patna University, Patna, Bihar, India

⁴Department of Physics, MANIT Bhopal, Madhya Pradesh, India

Abstract:- Using a high temperature solid state reaction approach with the carbonate of sodium metal and B_2O_3 as starting materials, the Sodium metaborate NaBO_2 have been produced. Pressed pellet of this compound, thermoelectric powers (S) and electrical conductivity (σ) is tested in the temperature ranging from the 440K to the melting point. Finding have been presented as plots of $\log \sigma T$ Vs T^{-1} and $\log S$ Vs T^{-1} . It is noted that at a certain temperature for the solid, σ jumps by a factor of 10 and reaches a value on the order of 3 around 1000K. For this solid S value exhibits an anomaly at the similar temp; this temp. is known as the phase transition temperature (T_P) of the solid. Utilizing a time dependency analysis of dc electrical conductivity, the ionic (σ_i) and electronic (σ_e) components of total conductivity have been assessed. It can be seen that the contribution of σ_i to σ is greater as compared to the 99 percent for the solid over T_P , and that below T_P , although it declines, it still more than 96 percent up to 500K. It has been determined, based on these findings, that this material can be found in two distinct phases. Above the transition point, the phase is superionic, and below the transition point, it is mixed conductor.

Keywords: Ionic conductivity, Electrical conductivity, Phase transition temperature, Thermo-electric Power, Electronic conductivity,

1. Introduction

Numerous researchers (1-28) have studied the electrical conductivity of some sodium-based salts in an effort to find sodium-ion conducting superionic solids, but no major attempt had been made in estimating the relative contribution of electronic & ionic conductivities in them, that is required to assess their capacity for use in electrochemical devices. Additionally, the majority of research on these mentioned compounds is restricted to either the phase of superionic, which is located slightly below the melting-point (2), or the low conduction of the β -phase (3-8). They haven't been thoroughly studied using a broad variety of temperatures (through their room temperature to the melting-point). Given the scarcity of research, we decided to re-evaluate this salt from the aforementioned perspectives. This research makes an effort in that approach by studying the solidified melt of NaBO_2 . Additionally, new findings on the electrical transport of sodium-based superionic solids have been presented. These results obtained are very useful to solid state alkali based rechargeable batteries. The next generation of solid-state rechargeable batteries uses very low cost, very safe batteries. Solid electrolytes from sodium sources are essential for enhancing the performance for the all batteries of solid-state. Due to the limited supplies of conventional fossil fuels, it is now essential to develop renewable energy sources like nuclear, solar, and wind (13). However, these renewable sources cannot provide a consistent supply of electricity since they are erratic in terms of time and location. As a result, goal has been changed towards the electrical storage of the energy to mitigate the intermittent nature of sources of the energy. A rechargeable battery may efficiently transform chemical energy into electrical energy by storing it (14). Rechargeable batteries have developed into an industrial product during the last 20 years, and they are now employed in portable energy storage systems and electrical vehicles, among other commonly used electronic goods. Energy storage from sources of the renewable energy, includes wind turbines & solar cells, is crucial. Therefore, rechargeable batteries are required to prevent climate change, a problem that affects the whole world today.

2. Objectives

The primary goal of researching sodium ion salts is to produce perfect, room-temperature sodium ion superionic solids. The best course of action in this regard, in my opinion, is to first investigate the electrical transport in a few sodium salts over a broad temperature range, ideally from room temperature to the solid's melting point, and attempt to comprehend the electrical transport mechanism in all phases. To accomplish this, you should then synthesize compounds using high-quality sodium ion conducting salts. In fact, research has been done on sodium ion conducting substances in a variety of states, including molten, slightly below melting temperature, and occasionally throughout the whole superionic phase. Few investigations in their typical (low temperature) phase have been published. A more comprehensive investigation of sodium salts from the normal to superionic phases could provide valuable insights into achieving room temperature sodium ion conducting solids. Sodium salts have often been the subject of specific research phases. Furthermore, in the majority of cases, there hasn't been a systematic evaluation of the ionic and electronic contributions to electrical conductivity, which is crucial to comprehending the material's transport mechanism as well as determining the material's potential for electrochemical applications. The paucity of research and the practicality of superionic solids based on sodium encouraged me to pursue these investigations.

3. Methods

Na_2CO_3 with stated 99.99% purity procured through the M/S rare and Research chemical Bombay, India and B_2O_3 (with stated 99.99% purity) procured through the M/S chempure, Calcutta, India. No specific chemical impurities have been given by the supplier within 0.01% and we have made no attempt to know them. Starting materials were divided into equal portions based on molecular weight, carefully mixed, and burned in air for 60 hours with one intermediate grinding. The firing temperature was 900K. On a solidified melt, electrical conductivity was measured. For this, a self-made sample holder was used. It is composed of a test tube with a flat bottom made of corning glass & two parallel, flat silver electrodes that are the same size and have the same surface area. Two substantial silver cables are used to link these two electrodes to the outside world. A sample container is filled with the substance whose conductivity has to be determined, then pressed. Then it is cooked until the salt within dissolves. It cools to room temperature gradually. The measurement device is then linked to the outside electrodes. Using the sample container and method described elsewhere, the measurement of σ was carried out (15-16).

4. Result

NaBO_2 produced in various batches have had their thermoelectric power S and electrical conductivity (σ) evaluated as temperature function. The measurements were taken throughout heating & cooling cycles respectively. No considerable variations has been noticed in S & σ value in the cooling and heating cycles. The findings have been given in the figure-1 as $\log \sigma T$ Vs T^{-1} & S Vs T^{-1} curves. Ion or electron migration, or perhaps both, contribute to electrical conductivity. The ionic and electronic contributions have quite distinct underlying hypothesis. Therefore, it is necessary to determine whether the conductivity is primarily ionic or electronic in order to give any relevant discussion of electrical conduction. There are standard ways to do this (17-18) but measuring σ_{dc} as a time function using an electrode that inhibits ionic but not the electronic conduction is a far simpler technique. If the electrodes being used to test this conductivity are able to stop the flow of ions, a time-dependent dc electrical conductivity will often be seen in solids with ionic conduction. Positive ions flow in the field direction whereas negative ions move in the reverse direction at the time when electric field has been applied to the two electrodes using a potential difference. Ions cannot discharge at electrodes because electrodes are impeding their passage, therefore they start to accommodate there instead. Thus, as more ions are unable to reach the electrode and as the d.c. source of current falls, the net force exerted on the ions seeking to flow in that direction diminishes. Over time, the opposing field tends to rise and eventually catch up to the applied field ($t \rightarrow \infty$). Therefore, the d.c. current in pure ionic solids declines with time and eventually tends to zero.

If the aforementioned argument is applied to the example of a mixed ionic conductor, one would anticipate a steady drop in the current that would eventually tend to reach a constant value. This current develops because the polarization caused by the ions prevents the electric field from being zero. When these transients have passed, the

remaining constant amount of current may be completely attributed to the electron (19-20). The transient is caused by ionic charges. The entire current produced by both ions and electrons is known as the initial current (current at $t=0$). Thus, we may assess the overall conductivity as well as the ionic and electronic components from time-dependent current measurement. At low but constant temperatures and electric fields, we conducted time-dependent research of σ . Figure displays typical plot (2). Plots with different temperatures are of a similar kind. The graphic shows that, generally, σ declines with course of time and has a tendency to remain constant. At lower temperatures, the tendency of consistency takes a little while to emerge, but it becomes stronger as the temperature rises. The electronic component (σ_e) of the conductivity is the constant value of $\sigma_{d.c.}$ over a long period ($t \rightarrow \infty$), and the value of $\sigma_{d.c.}$ for $t \rightarrow 0$ is the total conductivity (ionic + electronic). σ was tested at a few affixed frequencies to see whether $\sigma_{d.c.}(0)$ correlate to true conductivity. The results are shown in Fig3. This graphic demonstrates that there is no distinction between $\sigma_{d.c.}(0)$ and $\sigma_{a.c.}$ values. This leads one to believe that the samples do not have any holes in them and that the impacts of grain boundaries are not substantial. At each of the 6 or 7 broadly separated temperatures used in the time-dependence research of $\sigma_{d.c.}$, $\sigma_{d.c.}(0)$ and $\sigma_{d.c.}(\infty)$ were obtained. These numbers have been used to calculate the ionic ratio to electronic conduction ($r = \sigma_i / \sigma_e$) by utilizing this given relation

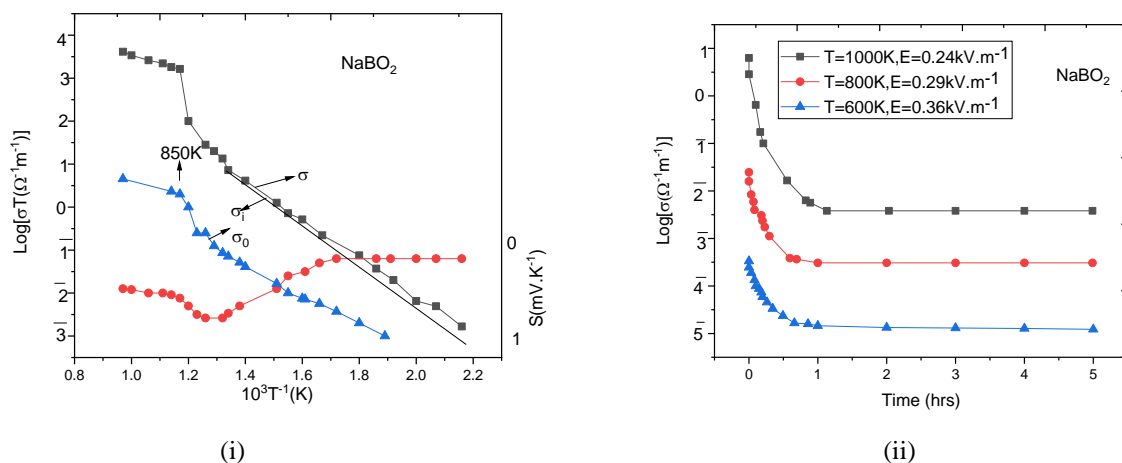
$$\begin{aligned} r &= \frac{\sigma_i}{\sigma_e} \\ &= \frac{\sigma - \sigma_e}{\sigma_e} \\ &= \frac{\sigma_{d.c.}(0) - \sigma_{d.c.}(\infty)}{\sigma_{d.c.}(\infty)} \end{aligned} \quad (1)$$

The graph in Figure 4 displays the $\log r$ against temperature. By applying the relation, one can estimate from this value the contribution of ionic & electronic conductivity for overall conductivity at the point of any given temp.

$$\sigma_i = \left(\frac{r}{r+1} \right) \sigma \quad (2)$$

$$\sigma_e = \left(\frac{1}{r+1} \right) \sigma \quad (3)$$

The proportion of electronic and ionic contribution to σ in the material under study at various temperature is shown in table-1 to further illustrate this (Fig-1). We have distinguished the conductivity through electronic (σ_e) and ionic (σ_i) components by utilizing the $\log r$ against plots of T . Their variation having the temperature displayed in Fig-1 For NaBO_2 as $\log \sigma_i T$ and $\log \sigma_e T$ against T^{-1} plots. Figures 1 depict their temperature fluctuation. NaBO_2 as plots of $\log \sigma_i T$ and $\log \sigma_e T$ against T^{-1} . It is more acceptable to give the analysis of these plots individually since the of electronic and ionic transportation theories are quite distinct from one another.



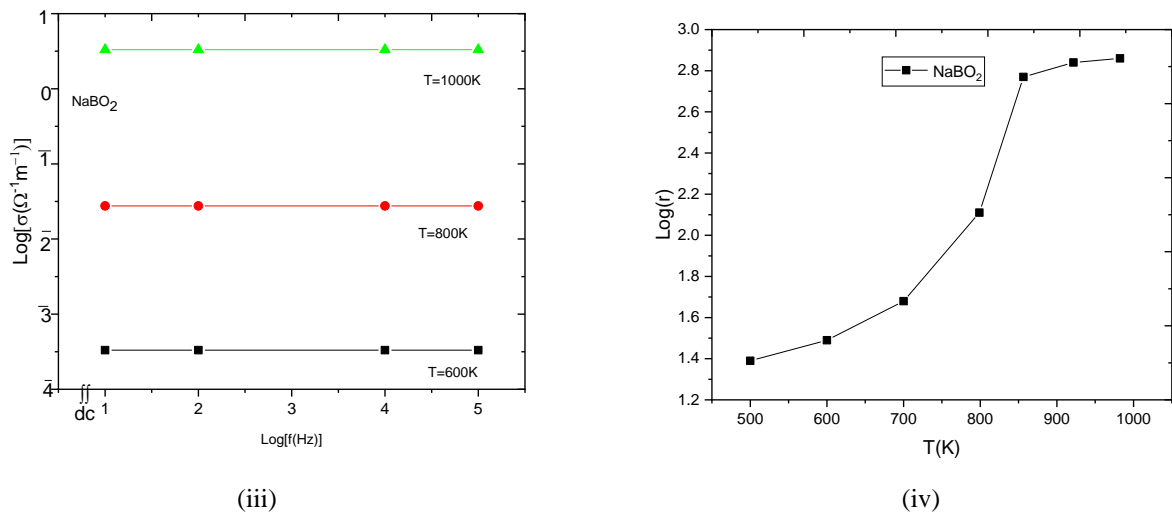


Fig. (i) Plot of Logarithm of the product of conductivity and temperature ($\text{Log } \sigma T$) and seebeck coefficients (S) Vs Inverse of temperature (T^{-1}); σ_i and σ_e curves are also shown. (ii) Plot of Logarithm of electrical conductivity (σ) Vs Time. (iii) Plot of Logarithm of electrical conductivity ($\text{Log } \sigma$) Vs Logarithm of frequency ($\text{Log } f$). (iv) Plot of Logarithm of ratio of ionic to electronic conductivity ($\text{Log } r$) Vs Temperature

Ionic Conductivity

The curve of $\text{Log } \sigma_i T$ Vs T^{-1} for the studied solid is given in Fig-1. These graph demonstrate that at higher temperatures, there has been essentially no variations among the σ and σ_i values, but at lower temperatures, there is a little difference.

In various temperature ranges, $\text{Log } \sigma_i T$ curves are typically linear and may be separated into 3 regions: (1) linear region below certain temp. $T < T_1$. (2) Non-linear regions for temperature $T_1 < T < T_2$. (3) Flat and linear regions $T > T_2$. Temperature T_1 , T_2 and T_3 are separate for the solid. The equations may be used to express the fluctuations of σ and S in these linear ranges.

$$T \sigma_i = C \exp\left(\frac{-E_a}{KT}\right) \quad (4)$$

and

$$S = \frac{\eta}{eT} + H \quad (5)$$

Where c is a constant that is unaffected by temperature, E_a denotes activation energy, η denoted as slope of the curve that plots S against T^{-1} , and H is a constant value. Table 3 presents the results of all of these measurements as their respective values

In the third temp. region, σ_i values are very high ($3.306 \Omega^{-1}\text{m}^{-1}$) and the energy of the activation not being large (0.35 eV) (Table3). Therefore, this is the superionic phase region of the given solid. σ values of this solid increase with temperature and reaches a value of $3.31 \Omega^{-1}\text{m}^{-1}$ at 850K. Above 850K hence is a bending of the $\text{Log } \sigma_i T$ Vs T^{-1} plots. Therefore, the real superionic phase of this material that could be employed for application purpose from 850 K to 1100K. The electronic conductivity in this given range is insignificantly small and thus both the σ & S must grow completely because of ions.

TABLE 1: Total conductivity (σ_T), Ionic conductivity (σ_i) Electronic conductivity (σ_e), and ratio of Ionic to electronic conductivity (r) at various temperature for NaBO_2 .

T(K)	$\sigma_T(\Omega^{-1}\text{m}^{-1})$	$\sigma_e(\Omega^{-1}\text{m}^{-1})$	$\sigma_i(\Omega^{-1}\text{m}^{-1})$	r	Log r	% σ_i
------	--------------------------------------	--------------------------------------	--------------------------------------	---	-------	--------------

1000	3.31	4.00×10^{-3}	3.3060	8.27×10^2	2.92	99.88
940	2.67	3.30×10^{-3}	2.6667	8.08×10^2	2.91	99.88
880	1.97	2.70×10^{-3}	1.9673	7.29×10^2	2.86	99.86
800	2.40×10^{-2}	1.90×10^{-4}	2.3810×10^{-2}	1.25×10^2	2.10	99.21
700	4.30×10^{-3}	8.40×10^{-5}	4.2160×10^{-3}	5.02×10^1	1.70	98.05
600	3.20×10^{-4}	9.60×10^{-6}	3.1040×10^{-4}	3.23×10^1	1.51	97.00
500	1.80×10^{-5}	6.70×10^{-7}	1.7330×10^{-5}	2.59×10^1	1.41	96.28

TABLE 2: Electrical conductivity at few fix temperature.

Compound	Electrical conductivity σ ($\Omega^{-1}\text{m}^{-1}$) at					
	500K	600K	700K	800K	900K	1000K
NaBO ₂	1.80×10^{-5}	3.20×10^{-4}	4.30×10^{-3}	2.40×10^{-2}	2.12	3.31

TABLE 3: Summnerized result of electrical conductivity (σ) of NaBO₂ compound.

Compound	Higher region Temperature ($T > T_2$)K		T_2 (K)	Lower region Temperature ($T < T_1$)K		T_1 (K)	T_c
	E_a (eV)	σ_0 ($\Omega^{-1}\text{m}^{-1}\text{K}$)		E_a (eV)	σ_0 ($\Omega^{-1}\text{m}^{-1}\text{K}$)		
NaBO ₂	0.35	1.94×10^5	880	0.87	5.57×10^6	820	850

TABLE 4: Summnerized findings of the thermoelectric power (S), changes along the temperature of the NaBO₂ compound.

Compound	Higher Temperature Region ($T > T_2$)			Lower Temperature Region					
				$T < T_1$					
				$T_1 > T > T_2^I$			$T < T_1^I$		
	η (eV)	H (mV K^{-1})	T_2 (K)	η (eV)	H (mV K^{-1})	η (eV)	H (mV K^{-1})	T_1 (K)	T_2 (K)
NaBO ₂	-0.32	-0.36	875	0.0	-0.96	0.13	-0.50	825	850

Thus the slope of S Vs T^{-1} plot in this region provides the transportation of heat ($Q \approx \eta$) for the ions of mobile and the log σ Vs T^{-1} plot slope, its activation energy ($E_a = hm$). It has been observed by the Tab.5 that hm is found slightly larger than Q . This suggest that extended lattice gas model is appropriate for the solid. This model takes the merit of all other models. In this model Q and hm are related by the equation (24)

$$hm = Q + hm' \quad (6)$$

and

$$hm' = \frac{q^2}{4\pi^2 a \epsilon_0} \left(\frac{1}{K_\infty} - \frac{1}{K_0} \right) \quad (7)$$

where

$$hm' = \frac{E_B}{2}$$

E_B denotes the polar ion binding energy, q signifies the mobile ion charge, a is its average separation, the permittivity constant ϵ_0 , K_0 & K_∞ are the static and optical dielectric constants, correspondingly, and a is the average distance between them. The hm' experimental values are also been presented in the table 5. And the span of superionic phase, melting point (T_M), transition temperature (T_C), thermoelectric power (S) & Electrical conductivity (σ) at 1000K of NaBO_2 compound is given in table 6.

TABLE-5: Mobile ion enthalpy (h_m), temperature dependent constants (C_2), mobile ion heat (Q) and constant (H) in superionic phase of NaBO_2 compound.

Compound	$h_m = E_a$ (eV)	$C_2 = \sigma_0 (\Omega^{-1} \text{m}^1 \text{K})$	$Q = \eta$ (eV)	H (mV K^{-1})	$H_m' = (h_m - Q)$ eV
NaBO_2	0.35	1.94×10^5	0.32	-0.36	0.03

TABLE 6: Span of Superionic phase (δT), Melting point (T_M), Transition temperature (T_C), thermoelectric conductivity (σ) and Electrical conductivity (σ) and thermoelectric power (S) at 1000K of NaBO_2 compound.

Compound	δT (K)	T_C (K)	T_M (K)	σ at 1000K $\Omega^{-1} \text{m}^{-1}$	S at 1000 K mV K^{-1}
NaBO_2	250	850	1100	3.31	-0.66

5. Discussion

The ionic and electronic contribution to total electrical conductivities has been obtained through the time dependent studies of dc electrical conductivity of the studied material. Ionic contribution to overall electrical conductivity has been shown to rise with temperature, although it stays below a critical temperature at less than 99%. However, at the critical temperature, its contribution abruptly rises and surpasses 99.8%. This demonstrates unequivocally that solid under investigation has 2 phases, one below and one above the critical temp. Consequently, the critical temp. might also be referred to as the temp. of the phase transition (T_P). With a 2–5% electronic contribution, ionic conduction dominates the phase below the transition temp. ($T < T_P$). Thus, this phase, which we refer to as the typical ionic phase, has mixed conduction. The electrical conduction of the phase which is above T_P is virtually entirely ionic, with practically little electronic input. We can call it superionic phase. Thus, the time dependent study of σ_{dc} itself shows that the studied solid have two phases. They have a phase in which entire contribution to electrical transport is due to ions. What are these mobile ions? To resolve this question, By looking at our data of thermoelectric power (S). Due to the fact that the thermoelectric power is always negative across the whole temp. range that was tested, the mobile carriers have a positive charge. 2nd kinds of +ve charged ions are there in NaBO_2 compound namely Na^+ and B^{3+} ions. B^{3+} ions are not likely to be moveable due to its higher +ve charge whereas Na^+ ions have been anticipated to have maximum mobility due to its low +ve charge and the size is small. Such ions often move across the environment through hopping. On the other hand, because of the high activation energy that is necessary, the intrinsic hopping conduction of such ions through one lattice site to another is an extremely unlikely occurrence (-5eV or more). Because electrical conductivity is high, it may be concluded that only one kind of charge carrier is accountable. The thermoelectric effect indicates a positive charge carrier nature. As a result, it seems that there are several Frankel defects present in the examined materials' normal ionic phase and that more may be produced at higher temperatures. The thermal development of a significant number of Frankel defects is less likely to occur at lower temperatures, or in the typical ionic phase,

since their formation requires more energy. As a result, below the temperature of the phase transition, their number largely stays constant. In a case like this the σT variations along the T that is presented below.

$$\sigma T = C_1 \exp\left(\frac{-h_f}{kT}\right) \quad (8)$$

where C_1 represents constants that are unaffected by temperature and h_f represents the enthalpy required for the mobile defects migration. Because of this, the slope that appears in linear plots of $\log \sigma T$ Vs T^{-1} below the temperature at which the phase transition appears, E_a , is in fact the enthalpy for the mobile defects migration (h_f). The results of this evaluation may be seen in Table-3 and $E_a = h_f$ is presented for the solid in the series that were under investigation. These are on the order of 0.8 eV, which is a value that is fairly acceptable for the migration enthalpy of Frankel defects.

There are a few different models that can be used to describe the superionic phase. The structural disorder model, the free ion model, the ionic polaron model, the lattice gas model, the extended lattice model, and others like them all play an important role in the literature to describe how the electrical transport mechanism works. They hypothesize that there is a connection between the heat of transport, denoted by Q , and the enthalpy involved in the mobile ions movement (h_m). After these given parameters have been discovered, one is able to make a prediction regarding the appropriateness of a specific model for the conduction of electrical current. This demands for homogenous thermoelectric power (S_{hom}) measurement, which in this situation translates to the measurement of S utilizing respective electrodes made of alkali metals. The observed thermoelectric voltage for other electrodes, however, includes a contribution due to the electrode-electrolyte interface's contact potential's temperature dependency. Because the temp. variation between the two phases during the S measurement is just -10 K, it is possible that this contribution is not a very significant one. Therefore, we can deduce that $S = S_{\text{hom}}$. If just one kind of ion is mobile, then the expression that describes the variation of S and can be written as follows: (25-26).

$$S = S_{\text{hom}} = \frac{Q}{eT} + H \quad (9)$$

and

$$T \sigma = C_2 \exp\left(\frac{-h_m}{kT}\right) \quad (10)$$

Where Q represents the mobile ion's heat & H represents a constant, C_2 represents a temp-dependent constant, and h_m represents the mobile ion activation enthalpy. We are able to determine the values of H , Q , h_m , and C_2 due to the linear nature of the plots of S and $\log \sigma T$ Vs T^{-1} Table 5 has these data in their respective columns. As can be seen from the chart, h_m is discovered to be slightly more than Q . This indicates that the extended lattice gas model can be successfully applied to solid. This model is superior than every other model in every respect.

Electronic conductivity

The $\log \sigma_e T$ - T^{-1} charts (Figures-1) for these materials are quite similar to the $\log \sigma T$ - T^{-1} plots. At the same temperature at which one finds a surge in, one also observes a jump σ in the electronic conductivity that is various orders of magnitude larger. We have referred this as the phase transition temperature. It would appear that a structural change takes place in these given solids when they are subjected to the temperature that causes the phase transition. Below the given temp, the $\log \sigma_e T$ - T^{-1} plot is linear, and it may be modelled utilizing the equation.

$$\sigma_e T = \exp\left(\frac{-W}{kT}\right) \quad (11)$$

W is the activation energy for electronic conduction, and σ_0 is a constant. Table-7 provides values for σ_0 , W and the phase transition temperature. This table shows that the values of W are high, but not high enough to be related to the solid's energy band-gap. The electrons hopping trapped at the center defects seems to be the cause of electronic conduction.

Table-7: consequences of the electronic component's contribution to the electrical conductivity of the NaBO₂ compound.

Compound	W(eV)	σ_0 ($\Omega^{-1}\text{m}^{-1}\text{K}$)	T_P
NaBO ₂	0.84	1.12×10^5	850 ± 5

6.Conclusion

The substance under investigation is a common superionic solid, and it exhibits a phase transition at a specific temperature known as the phase transition temperature (T_P). They exhibit conventional ionic solid behavior below T_P and superionic solid behavior above T_P , staying visible until their melting points. While the majority of electrical conduction in the normal ionic phase is ionic, the solid also contributes a sizable (1-4%) electronic contribution. Frankel defect is the primary cause of electrical conduction in the normal ionic phase. The solid under study experiences a phase shift from the conventional ionic phase to the superionic phase above T_P . Electrical conduction in the superionic phase is nearly ionic, with a very tiny ($<10^{-2}\%$) electronic contribution. A distinct indication of a phase transition has been detected in σ , S studies as an abnormality. The value of T_P observed from all these (σ , S) studies is nearly same, indicating same happening in the material.

7.Acknowledgement

Authors are thankful to university Grant commission, New Delhi for providing Financial Assistant as startup grant No-30-505/2020(BSR)

8.Declaration of Competing interest

No potential conflict of interest was reported by the author(s)

9.References

- 1 A. Benrath and K. Dreikopf, Z. Phys. Chem. 99 55(1921).
2. A. Kvist and A. Lunden, Z. Naturforsch. 20a ,235(1965).
3. I. D. Raistrick , C. Ho and R. A. Huggins , Mater. Res. Bull. 11 ,953(1976).
4. J. B. Boyce and J. C. Mikkelsen Jr, Solid State Commun. 31(1979) 741 (1979).
5. K. Singh and V.K. Deshpande, Solid State Ionics 13 , 157(1984).
- 6.H.B. Lal, K. Gaur and A.N. Thakur, J. Mat. Sci. lett. 10 ,1113-1115(1991).
- 7.M. Aniya Solid State Ionics 121 , 281(1999).
8. K.M. Mishra, A.K. Lal, F.Z. Haque, Solid State Ionics,167 , 137-146(2004).
9. S. Tripathi, K.M. Mishra, S.N. Tiwari Emerging material Research 1, 205-211(2011).
- 10.N. Singh, J. Bamne , K.M. Mishra, N. Singh, F.Z. Haque Emerging Trends in Nanotechnology, 279-307,(2021).
11. A. Manthiram ,JB. Goodenough . Nat Energy;6(3):323(2021).
12. R. Chopde, N. Singh, K.M. Mishra, J. Bamne, F.Z. Haque, Emerging material research 9(4), 1103-1112 (2020).
13. Z. Yang, J. Zhang, M.C. Kinmer-Meyer, X. Lu, D. Choi, J.P. Lemmon, J. Liu ,J.. Chem. Rev. 111 (2011)
14. M. Annand, J. M. Tarascon, Building better batteries, Nature 451 , 652(2008).
15. K. Shahi, H. B. Lal and S. Chandra, Ind. J. Pure Appl. Phys. 13 (1975) 1(1975).
16. M. Singh, Ph.D. Thesis D.D.U. Gorakhpur University, Gorakhpur, India (1994).
17. C. Tnbandt, J. Electrochem. Soc. 26 (1920) 358(1920).

18. Idem, in Handbuch der Experimental Physik, Band XII 1 Teil p. 383(1932)
19. C. C. Liang and L. H.N Barnette, J. Electrochem. Soc. 123 , 453(1976).
- 20.. A.J. Pathak, K. Gaur and H.B. Lal, J. Mater. Sci. Lett. 5, 785(1986).
21. M. J. Rice and W. L. Roth, J. Solid State Chem. 4 (1972) 294(1972).
22. C.P. Flynn, Oxford University Press, (1972).
- 23.W.J. Pardee and G. D. Mahan, J. Solid State Chem. 15 , 310(1975).
- 24.G.D. Mahan, Phys. Rev. B14 , 780.(1976).
25. S. Chandra and J. Rolfe, J. Can, J. Phys. 48 ,397(1970).
26. S. Chandra, S.K. Tolpadi, and S.A. Hashmi, Solid State Ionics 28-30 ,651(1988)
27. S. Chandra, North Holland, Amstordam, (1981).
28. S. Chandra, S.A. Hashmi, M. Saleem, and R.C. Agrawal, Solid State Ionics 67 1(1993).